HYDROLOGICAL PROCESSES
Hydrol. Process. **28**, 5755–5768 (2014)
Published online 22 October 2013 in Wiley Online Library
(wileyonlinelibrary.com) DOI: 10.1002/hyp.10081

The impact of the South–North Water Transfer Project (CTP)'s central route on groundwater table in the Hai River basin, North China

Aizhong Ye,[1]* Qingyun Duan,[1] Wei Chu,[2] Jing Xu[1] and Yuna Mao[1]

[1] *College of Global Change and Earth System Science, Beijing Normal University, Beijing 100875, China*
[2] *Department of Civil and Environmental Engineering, University of California, Irvine, CA, 92617, USA*

Abstract:

The central route of the South–North Water Transfer Project (CTP) is designed to divert approximately 9.5 billion m^3 of water per year from the Han River, a major tributary of the Yangtze River, to the Hai River basin in the north China. The main purpose of this study is to assess the impact of CTP on groundwater table in the Hai River basin. Our study features a large-scale distributed hydrological model that couples a physically based groundwater module, which is sub-basin-based, with a conceptual surface water module, which is grid-based. There are several grids in each sub-basin and water exchange among grid that are considered. Our model couples surface water module and groundwater module and calculates human water use at the same time. The simulation results indicate that even with the water supply by CTP, the groundwater table will continue to decline in the Hai River basin. However, the CTP water can evidently reduce the decline rate, helping alleviate groundwater overexploitation in Hai River region. Copyright © 2013 John Wiley & Sons, Ltd.

KEY WORDS groundwater table decline; coupled distributed surface-groundwater hydrological model; the central route of the South–North Water Transfer Project

Received 15 January 2013; Accepted 30 September 2013

INTRODUCTION

The water resource distribution in China is highly uneven, with over 2000 m^3 per capita for southern China and only approximately 300–620 m^3 per capita for northern China (Xia and Chen, 2001). The situation has been made even worse by the climate change trends over the last 40 years. Since 1970s, both precipitation and run-off have increased in south China and declined in north China (Xu *et al*., 2010). In the Hai River basin, the annual total natural water supply (i.e. precipitation minus evapotranspiration) is less than 30 billion m^3, whereas the annual water usage by 123 million people in the region is approximately 40 billion m^3, resulting in a water shortage of 10 billion m^3 per year (Bulletin of Water Resources in China, 1999–2005). Over the past 50 years, groundwater has been increasingly exploited for domestic and agricultural use in the Hai River basin. A total of 89.58 billion m^3 of groundwater was extracted from 1958 to 1998 in the region (not including the Tuhaimajia River basin), comprising 47.1 billion m^3 from shallow aquifers and 42.5 billion m^3 from deep aquifers (Liu *et al*., 2010). In the Beijing region, part of the Hai River basin, the groundwater table has steadily receded from an average of 10 m below the surface in 1975 to over 35 m in 2005 (Xia *et al*., 2004; Stone and Jia, 2006; Xia *et al*., 2007).

To mitigate the water shortage in north China, the Chinese government has embarked on a massive engineering project to transfer water from southern China (Yangtze River) to northern China (Yellow River and Hai River basins). There are three routes planned to transfer water from the south to the north: the eastern, central and western routes. The central route of the South–North Water Transfer Project (CTP) is designed to move water from the Danjiangkou Reservoir on the Han River, a major tributary of the Yangtze River, to the Hai River basin. CTP is expected to move 9.5 billion m^3 a year when it is fully functional by approximately 2014 (You *et al*., 2011).

The water relocated through the CTP is expected to have a significant impact on the water resources in the Hai River basin (Liu and Zheng, 2002; Chen and Xie, 2010), especially on the groundwater reserves (Zhong *et al*., 2010). Water from the CTP will allow more recharging of groundwater from precipitation, which, in turn, will alleviate the decline of groundwater table in the area; in

*Correspondence to: Aizhong Ye, College of Global Change and Earth System Science, Beijing Normal University, Beijing 100875, China.
E-mail: Azye@bnu.edu.cn

other words, groundwater pumping will decline once the CTP is in operation. To evaluate the impact of the water relocation on groundwater table, quantitative tools must be employed. The Groundwater Modeling System (Cui *et al*., 2009; Shao *et al*., 2009; Zheng *et al*., 2009) software has been used to simulate the groundwater table change in the Hai River plain. The previous studies assume a decrease in population or groundwater pumping after CTP begins operating and claim that the groundwater level will recover. The groundwater table in the depression cone in Shijiazhuang is expected to recover by 2.1 m/a, and 0.8–1.5 m/a in Dezhou (Cui *et al*., 2009) after CTP begins operating. However, the surface hydrological process model is very simple in the Groundwater Modeling System and does not consider the impact of CTP on the surface water, resulting in large uncertainty in the simulation results. To accurately assess the CTP impact, we fully employ surface water and groundwater models (GWMs) in this study.

As early as in the 1970s, researchers began to use physically based GWMs to study the impact of groundwater pumping on water table (Garay *et al*., 1976; Cunningham and Sinclair, 1979). One of the most popular models, MODFLOW, developed by the US Geological Survey, is a three-dimensional finite-difference GWM. MODFLOW has been widely used because of its robustness and modular, adaptable concept (Barthel *et al*., 2005; Lubczynski and Gurwin, 2005; Liu *et al*., 2008). However, the standard MODFLOW is not capable of simulating the surface water–groundwater interaction at catchment scale. Many modified MODFLOW or coupled models have therefore been proposed. York *et al*. (2002) developed a coupled land–atmosphere model (CLASP II) that contains a full three-dimensional GWM and has the ability to represent the aquifer–stream interaction in a physically based manner. Rodriguez *et al*. (2008) integrated HEC-RAS and MODFLOW to improve the representation of hydraulic profiles in drain channels within a regional groundwater flow system. MT3DMS (a modular three-dimensional multispecies transport model) and MODFLOW have been coupled and applied to several areas (Lautz and Siegel, 2006; Wondzell *et al*., 2009). However, some research institutions traditionally perform surface water and groundwater research work separately. Surface water models (SWMs), including SWAT (Arnold and Williams, 1997) and the Xinanjiang model (Zhao, 1992), are based on the landform of a basin (Beven, 2001), whereas GWMs are based on geological and hydro-geological attributes, such as aspect of terrain, infiltration rate and specific yield. A research region maybe composed of many grids, and water level is calculated by the Boussinesq equation in every grid in MODFLOW (Harbaugh and McDonald, 1996). The different approaches of SWMs and GWMs cause problems in coupling them: (1) Scale problem; SWMs are based on large-scale grids or sub-basins, whereas GWMs are based on small-scale grids. (2) Flow direction; the flow direction in SWMs is decided by landform, whereas GWMs use three-dimensional flow. Therefore, how to calculate the hydraulic interaction between groundwater and surface water and how to achieve calculation synchronization pose great difficulties (Fleckenstein *et al*., 2010)

To resolve these problems, some coupled SWM and GWM models were developed, which can be divided into three types: (1) Independently developed model. The SWM only works for soil moisture and unsaturated zone water movement, and a simplified GWM is used, such as the Xinanjiang model and SWAT, which hardly think about ground water. The groundwater model only works for groundwater movement; the model input of surface water was from statistical models, such as MODFLOW. (2) Half-coupled model. On the basis of existing surface water and groundwater models, two models are coupled by scale switching. The calculation is performed by synchronization, so the model system becomes a two-way coupling system. However, there are some insufficiencies in interaction, such as in SWAT-MODFLOW (Kim *et al*., 2008) and CLM.PF (Maxwell and Miller, 2005). (3) Fully coupled model. Surface water and groundwater equations were coupled simultaneously.

If SWM and GWM are run independently, data exchange will be difficult, and the interaction between surface water and groundwater cannot be shown. A fully coupled model is feasible in theory, but it is difficult to implement in a large basin. Because high-resolution ground soil texture and rock attribute data are rarely observed in large basins, low-resolution data are usually used and cause large errors in the model. The current research concludes that the half-coupled model is a good choice and can obtain better simulation results.

The organization of the paper is as follows: The Introduction section and APPENDIX A describe a large-scale distributed hydrological model; Methods section introduces the data and study domain; section on Results and Discussion presents results and a discussion and Conclusions section provides conclusions.

METHODS

The area of Hai River basin is very large, so it is difficult to apply a complex model, such as MODFLOW, to the whole basin. Furthermore, it is impossible to obtain high-resolution groundwater parameters for MODFLOW in such a large basin. Therefore, we developed a large-scale distributed hydrological model that couples a physically based groundwater module with a conceptual surface

water module to assess the impact of CTP on the groundwater table in the Hai River basin.

Coupled structure of the model

The SWM is calculated on sub-basins, whereas the GWM is calculated on grids. Each sub-basin is composed of several grids (Figure 1). The GWM calculates each grid's hydraulic movement process when the SWM calculates the surface water process in a sub-basin. The SWM calculates the run-off process, the domestic water use, the industrial water use, the agricultural irrigation water use, the water transfer, the reservoir operation, the routing process and the groundwater pumps in each sub-basin (Figure 1). The GWM calculates the hydraulic movement process, the groundwater balance, the groundwater table change and the exchange between groundwater and surface water in each grid. Firstly, the possible water supply for groundwater based on surface water balance is obtained. Then, the groundwater balance is computed, and the water supply for the surface water from the groundwater is obtained by calculating the groundwater table. In other words, groundwater will supply surface water when the groundwater table is greater than elevation.

Calculation steps:

1) Surface run-off
2) Surface soil water movement
3) Infiltration of surface soil moisture
4) Unsaturated zone water movement
5) Groundwater movement
6) Routing and water use (human activity)

Surface run-off and surface soil water movement are calculated according to the landform in the sub-basin. Then, the infiltration water in the unsaturated zone is calculated. The unsaturated zone is marked off by numerous sub-layers according to the whole thickness (each sub-layer is 1 m in the current model). The infiltration and soil moisture change processes are calculated by Darcy's law and the Clapp and Hornberger (1978) equation. The precipitation supply for groundwater is then calculated. Finally, the groundwater movement process is simulated by solving the Boussinesq equation in the grids. Consequently, the groundwater table in each grid and sub-basin is obtained. (Figure 2). In this case, the surface water sub-basin area is greater than groundwater grid, and each sub-basin is composed of several grids. So, groundwater table of the sub-basin is average groundwater table of all grids in the sub-basin. The groundwater pump is an important water exchange method. In the Distributed Time-Variant Gain Hydrological Model, the detail groundwater pump is calculated through the following steps: firstly, the SWM calculated the water demand in each sub-basin; secondly, SWM calculated the water supply capacity from rivers and reservoirs; thirdly, if the water supply capacity was less than the water demand, the SWM obtained the possible groundwater pump in each sub-basin, which is the difference between water demand and water supply capacity; finally, the possible groundwater pump was divided equally to each groundwater grid in the sub-basin in GWM, the groundwater pump was the minimum value between the possible groundwater pump and the groundwater capacity in GWM.

Human activities, including irrigation, domestic and industrial water uses, are calculated in the model. At first, the model calculates human water use amount at each time step in each sub-basin, and then, the water is drawn from river, reservoir and groundwater (Figure 2).

The main features of the large-scale distributed hydrological model are presented in APPENDIX A of this paper.

The SWM was run for 1279 sub-basins in the Hai River basin, and the GWM was run at 500× 500 m resolution. There is a piedmont supply if the sub-surface run-off from a hill recharges the groundwater of the plain region (Figure 3) and a river supply if a river exists in the grid.

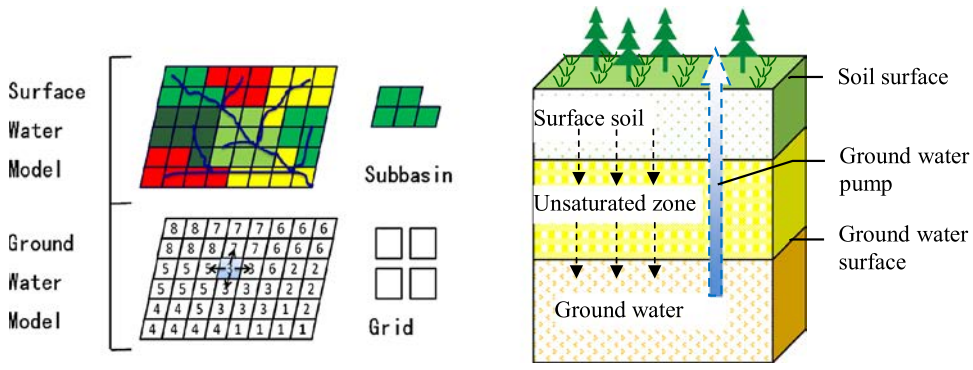

Figure 1. The coupled surface water and groundwater model in Distributed Time-Variant Gain Hydrological Model. Surface water model is based on sub-basin. Each sub-basin is composed of many fine resolution grids. The surface soil layer is less than 2 m deep. Surface run-off and sub-surface run-off occur in this layer. The unsaturated zone layer is between the surface soil and groundwater table, and the layer thickness changes from 0 to 100 m depending on the groundwater table. The groundwater layer is the aquiferous layer of groundwater

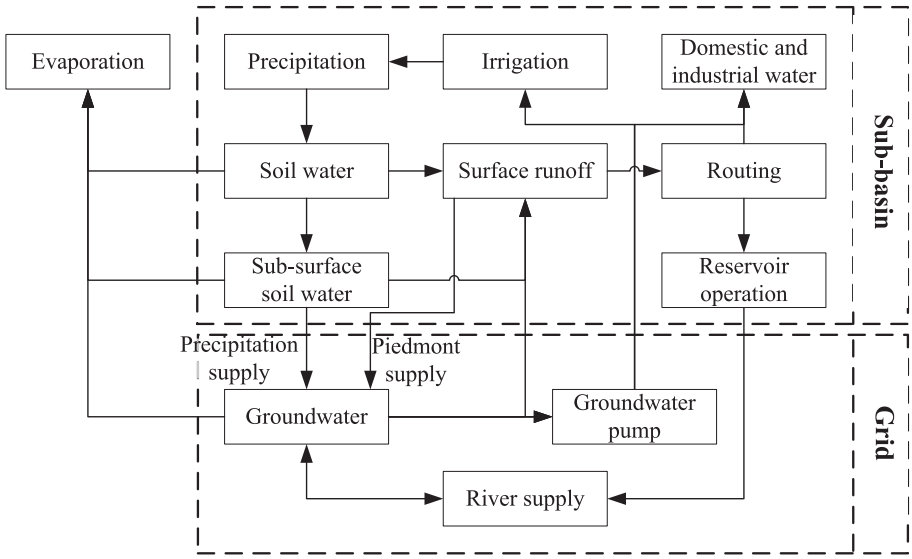

Figure 2. Flow chart of the Distributed Time-Variant Gain Hydrological Model. Surface

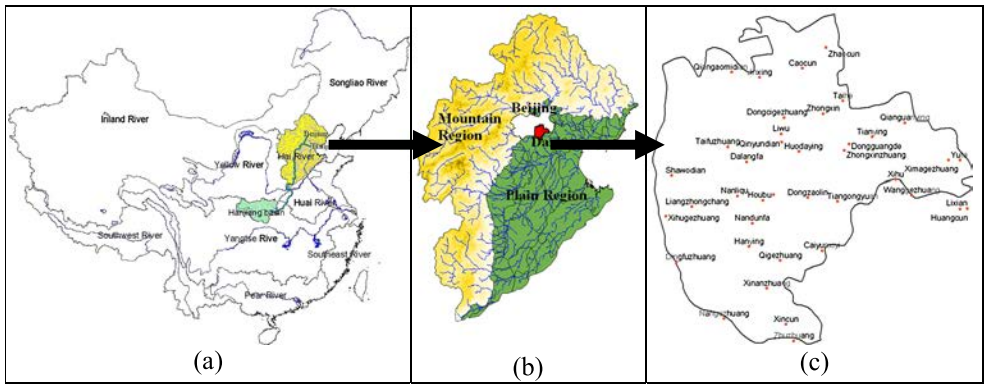

Figure 3. Location of the Hai River basins. (a) The central route of the South–North Water Transfer Project in China, (b) Hai River basin and (c) Daxing District of Beijing city. Points are observed wells in (c)

Model calibration strategy and criteria

The SWM and GWM were calibrated simultaneously in the coupled model. Surface water and groundwater are always being exchanged at any time. Therefore, we need to calibrate the SWM and GWM at the same time.

The performance measures include the Nash–Sutcliffe efficiency (NSE) value, *NSE*, correlation coefficient, *R*, and water balance coefficient, *B*, which are computed as follows:

$$NSE = \left[1 - \frac{\sum (Q_C - Q_O)^2}{\sum (Q_O - \overline{Q_O})^2}\right] \times 100\% \quad (1)$$

$$R = \frac{\sum (Q_c - \overline{Q}_c)(Q_o - \overline{Q}_o)}{\sqrt{\sum (Q_c - \overline{Q}_c)^2 \sum (Q_o - \overline{Q}_o)^2}} \quad (2)$$

$$B = \frac{SR}{OR} \quad (3)$$

where $Q_O, Q_C, \overline{Q_O}, \overline{Q_c}$ are observed value, simulated value, average observed value and average simulated value (m^3/s) respectively; *SR* is the sum of the simulated value (m^3/s); *OR* is the sum of the observed value (m^3/s). For *E* and *R*, the larger the values, the better the model performance. The perfect value for both measures is 1. For *NSE*, a negative value implies that the model performance is worse than the long-term average. The perfect value for *B* is 1. A value of less than 1 or greater than 1 means underestimation or over estimation respectively.

Study site and data compilation

The Hai River Basin has an area of 318 000 km^2 and a population of over 123 million. The annual precipitation ranges from 379.2 to 583.3 mm, approximately 75% of

which falls in the rainy months of June–September. The average annual temperatures in the catchment are between −4.9 and 15.0 °C (Yang and Tian, 2009).

The central route of the CTP runs from the Danjiangkou Reservoir on the Han River, a tributary of the Yangtze River, to Beijing, with 1246 km total channel distance. Seventy-one outlets are designed on the route from Hubei province to Beijing (Figure 3). The CTP will benefit 20 large cities and 100 counties. CTP covers a total area of approximately 155 000 km^2 and crosses approximately 200 river channels or canals (Wei *et al*., 2010).

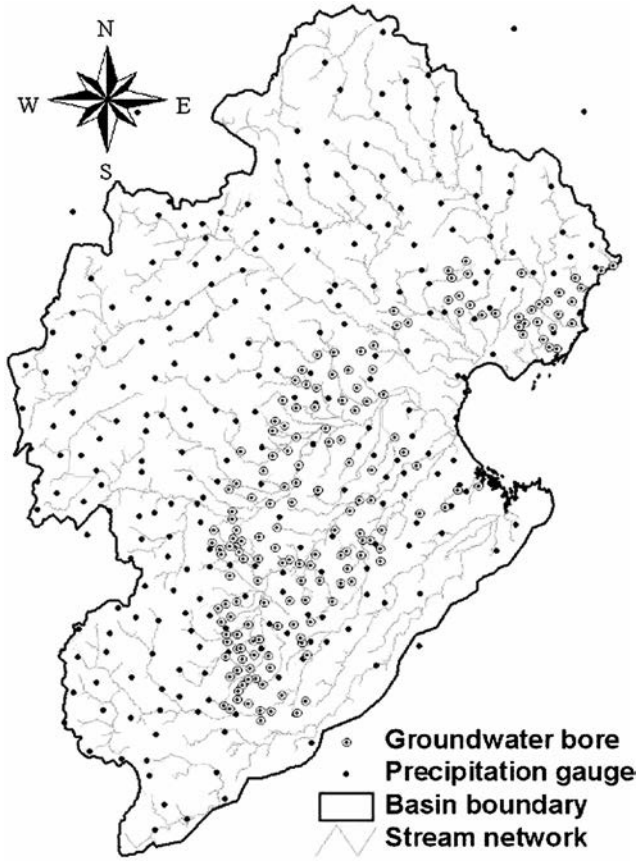

Figure 4. Precipitation gauges and groundwater bores in the Hai River basin

In the Hai River basin, there are 285 rain gauges (Figure 4) with daily precipitation data from 1995 to 2005 (Figure 7), 56 national weather stations providing daily temperature and pan evaporation data from 1956 to 2009 and 171 groundwater measuring wells (Figure 4).

To validate the groundwater model using point data, we obtained groundwater level observed data from 1999 to 2005 in the Daxing District of Beijing city, which was measured every 5 days. The Daxing District is located in the south of Beijing city and has an area of 1030 km^2 and a cultivated area of 422 km^2. There are 39 observation wells in Daxing District (Figure 3).

RESULTS AND DISCUSSION

Summary of model parameters

The GWM is very computationally demanding, requiring more than 5 h to simulate the period 1999–2005. Consequently, it is infeasible to obtain optimal parameters using auto-calibration algorithms. Therefore, we estimated the parameter values on the basis of physical mechanisms and experiments. Table I shows the SWM parameters, and Figure 5 shows the groundwater parameter.

Validation of groundwater level using point data

The wells are in the no. 290 sub-basins of the model in the Daxing District of Beijing city. The observed data are point data, but the corresponding model unit is a 500× 500-m grid. To validate the model, we compared the average observed groundwater level with the modelling result in the Daxing District of Beijing city, China. Because we cannot obtain each grid or sub-basin groundwater level, we only obtained several wells' groundwater level data in the Daxing District. We calculated the average observed groundwater level by using wells data and average simulated groundwater level with grids data in the Daxing District.

As shown in Figure 6, the observed level and simulated level closely match from 1999 to 2005. The Nash efficiency coefficient is 0.81, the correlation coefficient is 0.92 and the balance coefficient is 1.02. The curve of

Table I. Model parameters and their ranges

Parameter	Optimal value	Range	Unit	Remark
g1	0.4	0–1	/	Equation (A.2), run-off parameter
g2	3	1–5	/	Equation (A.2), run-off parameter
kr	0.01	0–1	/	Equation (A.2), run-off parameter
kg	5	1–10	/	Equation (A.2), run-off parameter
fc	5	0–200	mm/h	Equation (A.2), the soil permeability coefficient
n	0.3	0.01–0.5	/	Equation (A.4), Manning roughness coefficient

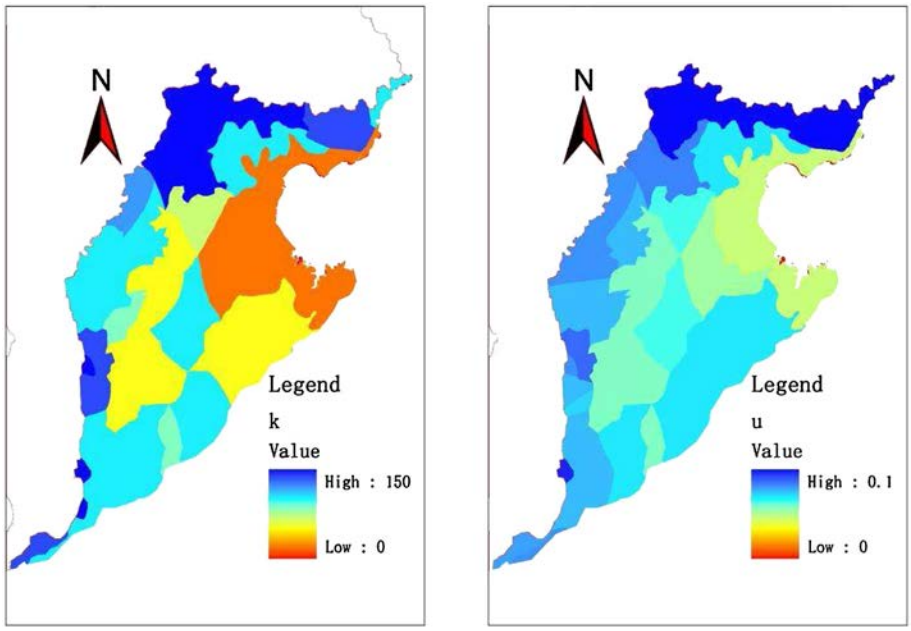

Figure 5. Groundwater parameters in the plain zone of the Hai River basin. k is the average hydraulic conductivity (m/day), and u is the specific yield (m^3/m^3)

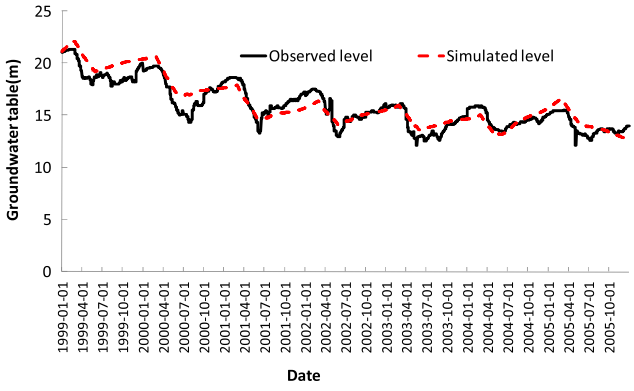

Figure 6. Average daily groundwater table in the Daxing District of Beijing city, China

the simulated level is smoother than that of the observed level because the groundwater pump is anomalous. However, the model only gives a rule to pump water. The rule is that the groundwater will be pumped if the surface water is not enough for water use (domestic, industry and agriculture).

Simulation of groundwater depth in the Hai River basin

Terrain and bedrock can affect the groundwater level. The spatial distribution of the groundwater level is highly heterogeneous in a large basin. However, the groundwater depth is less heterogeneous than the level. Because our aim is to study the water resource, we focus on the spatial and temporal depth changes.

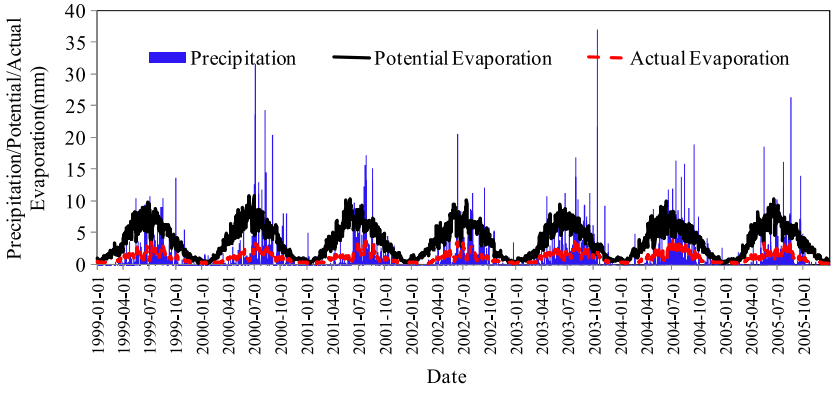

Figure 7. Daily precipitation/potential/actual evaporation processes in the Hai River basin

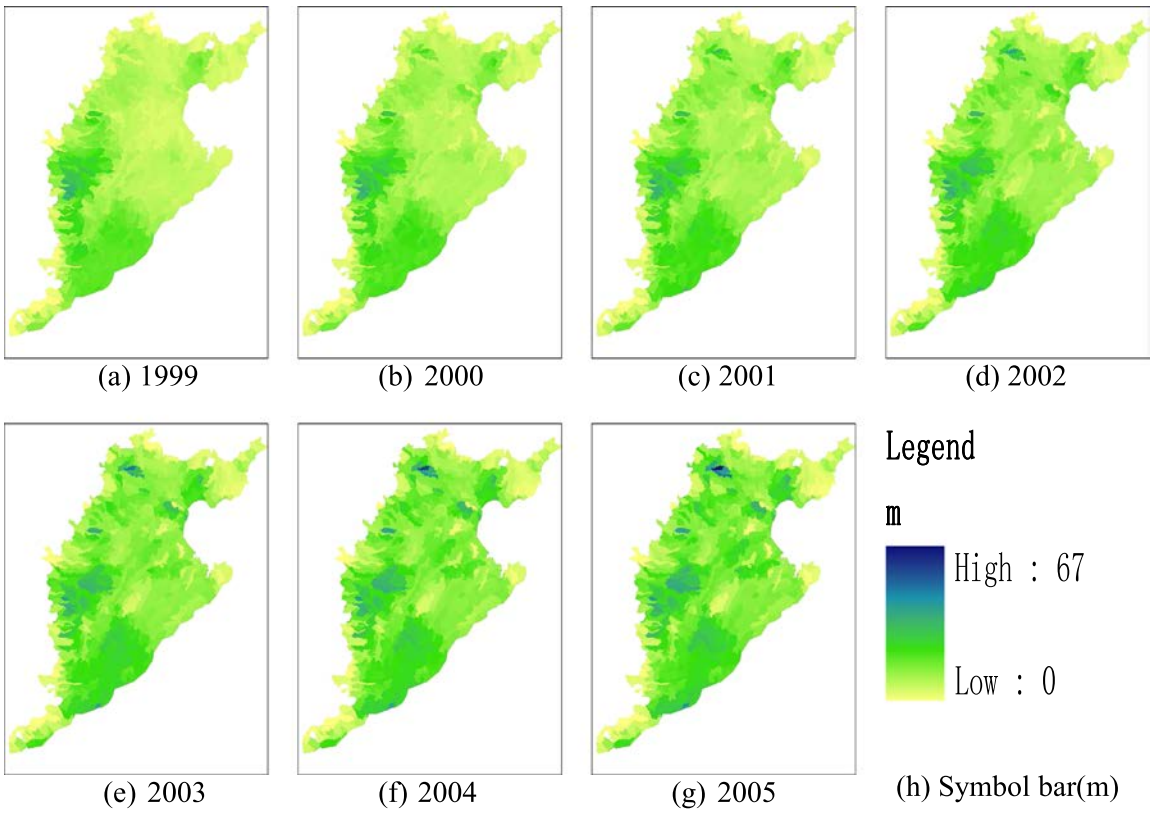

Figure 8. Simulated annual water table depth in the Hai River plain region (spatial resolution: 500× 500 m)

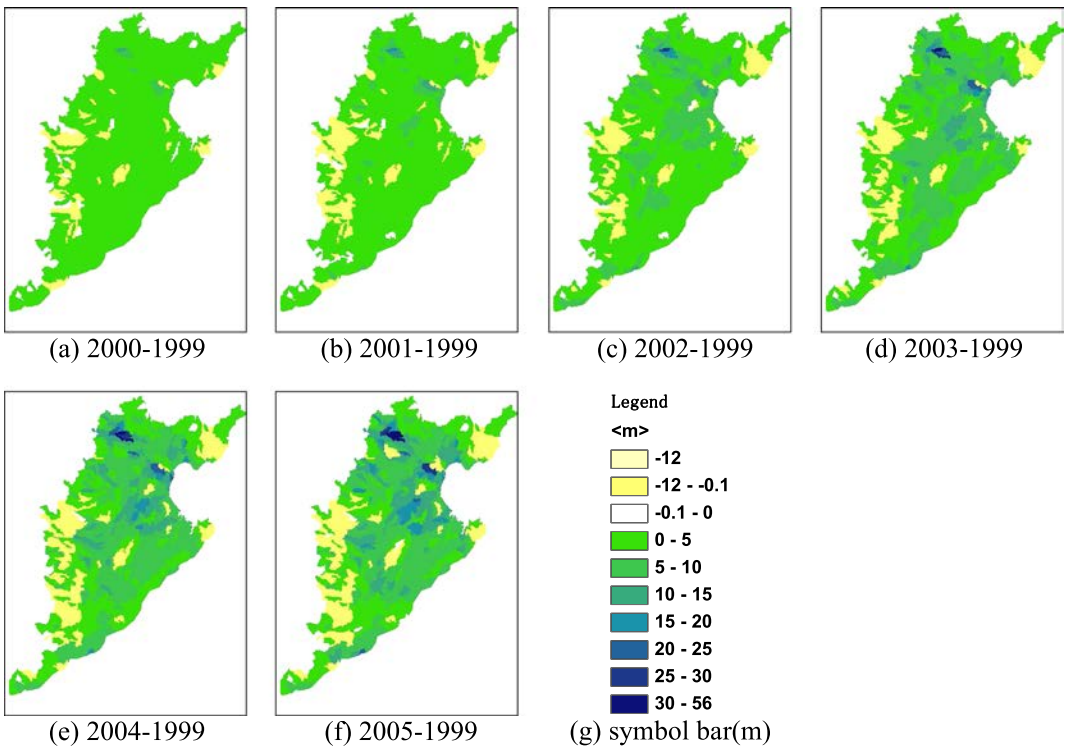

Figure 9. Simulated annual water table depth change relative to1999 in the Hai River plain region

The annual precipitation was 405 mm/year in 1999–2005, which is less than the historical annual precipitation. The annual actual evaporation was 415 mm, which is more than the annual precipitation due to the overexploitation of groundwater (see Figure 7). So the groundwater level continued to decrease.

The distributed hydrological model can give the spatial–temporal distribution of all hydrological factors. Figure 8 shows the groundwater depth from 1999 to 2005. Because of the pump over-supply, the spatial–temporal distribution of the groundwater depth has changed. The groundwater level declined in the whole basin, and the position of the groundwater funnel has moved. Perhaps the position of the groundwater funnel could not fully match the observed position because the model did not consider the actual position of the pump in detail.

Figure 9 shows that the groundwater depth increased in more than 80% of the Hai River plain region without transferred water, with rapid increases in large cities such as Beijing and Tianjin. Industry and domestic water uses are concentrated in the urban areas. The groundwater funnel area is enlarged. In many city zones (Beijing, Tianjin, Shijiazhuang etc.), groundwater depths increased more than 20 m.

Validation and analysis of water resource

The model calculated the water consumption and groundwater flow on the basis of the 1999–2005 observed data, and then, the results were compared with observed data in a water resource bulletin (Table II). The precipitation of the model is from spatial interpolation of rain gauge and meteorological station data. There is a close match in the water use and groundwater pump between the simulated results and water resource bulletin data in 1999–2005 (Table III). Therefore, we conclude the model is reasonable.

The water resource bulletin data and simulated results show that the water demand is greater than the natural water supply (Tables II and III), which is the main cause of overexploitation of the groundwater and decline of the groundwater level. The annual shortage of water supply is

Table II. Water resource bulletin of Hai River basin (billion m^3)*

		Water Resource					Water supply		
Year	Precipitation	Ground water	Surface water	Overlap water	Total water	Absence water	Total water	Surface water	Ground water
1999	122.45	17.23	9.20	7.05	19.38	23.77	43.15	16.27	26.88
2000	155.93	22.20	12.52	7.85	26.87	13.19	40.06	13.78	26.28
2001	132.48	17.46	8.97	6.42	20.01	19.19	39.20	12.43	26.77
2002	127.38	14.63	6.32	5.14	15.81	**24.17**	39.98	12.95	27.03
2003	186.29	25.29	13.08	6.35	32.02	5.68	37.70	11.56	26.14
2004	172.24	23.80	13.79	7.61	29.98	6.82	36.80	12.10	24.70
2005	155.85	21.55	12.19	6.99	26.75	11.3	38.05	12.76	25.29
Annual	150.37	20.31	10.87	6.78	24.40	14.88	39.28	13.12	26.16

*The groundwater overlaps part of surface water when we calculate the water resource. The bold text shows the maximum absence water.

Table III. Calculated groundwater resource from1999 to 2005 in the Hai River basin without water transfer (billion m^3)

	Supply				Calculated water use				Observed water use		
	Precipitation	River	Piedmont	Calculated pump	Domestic	Industry	Agriculture	Observed pump	Domestic	Industry	Agriculture
Annual	10.89	2.39	0.22	26.10	5.35	6.23	27.20	26.16	5.26	6.17	27.63
1999	8.49	1.79	0.24	30.21	5.39	6.27	29.61	26.88	5.15	6.91	30.72
2000	12.67	2.79	0.22	28.85	5.34	6.23	26.84	26.28	5.18	6.58	28.07
2001	11.44	2.33	0.21	24.99	5.32	6.19	27.64	26.77	5.18	6.23	27.80
2002	7.28	2.21	0.21	26.22	5.34	6.21	25.76	27.03	5.15	6.18	28.65
2003	12.57	3.08	0.23	25.40	5.35	6.22	25.41	26.14	5.35	5.97	26.19
2004	14.73	2.76	0.24	21.80	5.38	6.25	26.48	24.70	5.25	5.658	25.61
2005	9.06	1.76	0.22	25.24	5.34	6.21	28.69	25.29	5.55	5.67	26.37

Observed data are from the water resource bulletin of Hai River basin.

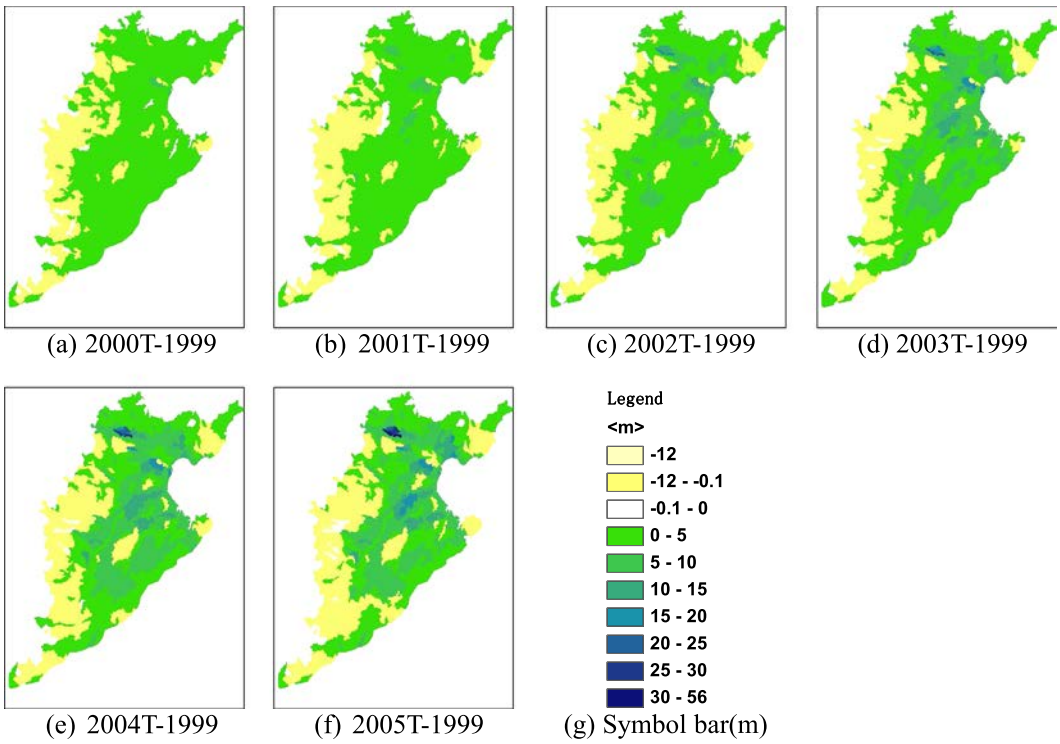

Figure 10. Simulated annual water table depth change relative to1999 in the Hai River plain region after transferring 9.5 billion m^3 water. 'T' after the year refers to 'water transfer'

Table IV. Calculated groundwater resource change from1999 to 2005 in the Hai River basin without water transfer (billion m^3)

	Calculated supply				Calculated water use		
	Precipitation	River	Piedmont	Calculated Pump	Domestic	Industry	Agriculture
Annual	0.264	0.094	0.108	−5.465	0.013	0.015	0.273
1999	0.099	0.856	0.051	−3.943	0.009	0.009	0.066
2000	0.251	0.448	0.101	−3.902	0.021	0.018	0.47
2001	0.245	0.369	0.118	−5.848	0.007	0.007	0.159
2002	0.217	0.197	0.12	−6.19	0.02	0.026	0.4
2003	0.399	−0.27	0.119	−5.087	0.014	0.02	0.315
2004	0.394	−0.533	0.12	−5.909	0.004	0.003	0.289
2005	0.246	−0.405	0.127	−7.376	0.016	0.023	0.214

Table V. Groundwater depth change relative to1999 in the Hai River plain region

		2000	2001	2002	2003	2004	2005
Min (m)	No transfer	−4.35	−7.62	−8.34	−9.05	−9.86	−11.40
	Transfer	−6.37	−10.59	−13.42	−15.49	−17.23	−18.48
Max (m)	No transfer	10.12	19.61	28.80	37.64	46.34	55.25
	Transfer	6.55	9.76	15.33	20.82	25.98	31.14
Mean (m)	No transfer	1.33	2.11	3.13	4.24	4.80	5.31
	Transfer	0.74	1.12	1.63	2.25	2.31	2.13
↑ Area (%)	No transfer	11.72	15.40	13.74	12.90	16.28	18.29
	Transfer	28.49	30.23	30.39	29.59	32.02	36.85
↓ Area (%)	No transfer	88.28	84.60	86.26	87.10	83.72	81.71
	Transfer	71.51	69.77	69.61	70.41	67.98	63.15

↑Area is the percentage of the region in which the groundwater level rises.
↓ Area is the percentage of the region in which the groundwater level declines.

14.88 billion m^3, whereas the greatest shortage was 24.17 billion m^3 in the year 2002.

Thanks to the government and citizens' efforts to conserve water, the total water use has been stable in the past 10 years. However, as population in cities, and industry and agriculture productions continue to increase, water demand will increase in the future, and we have to transfer water from other basins.

Impact of the CTP on groundwater

Natural water resources are not enough to meet the demand in the Hai River basin, and the demand outpaces the groundwater pumping rate. Without the transfer of water from other basins, there would be a water crisis. On the basis of the hydrological model, we propose a hypothesis that the CTP water will be distributed to the nearest several sub-basins of the rivers near each outlet according to the programming of the CTP. Then, the CTP water will enter the water cycle of the intake area. People will take water from the nearest sub-basins' rivers, reservoirs and groundwater for domestic, industrial and agricultural uses.

We use the model to quantitatively analyse the impact of CTP on groundwater. CTP plans to transfer a water discharge of approximately 300 m^3/s and an annual water supply of 9.5 billion m^3. Approximately, 6.5 billion m^3 (205 m^3/s) of water can reach the Hai River basin, of which 2 billion m^3 can reach Beijing and Tianjin city. The model supposes a transfer discharge of 300 m^3/s.

From Figure 10, we can see that the groundwater level will increase in approximately 30% area of the region after the water is transferred, but the groundwater level will continue to decline in approximately 70% area of the region (Table V). The simulated results show that CTP water cannot satisfy all requirements.

It is apparent that the groundwater depth without transferring water is lower than that with transferring water in the whole Hai River plain region. CTP can

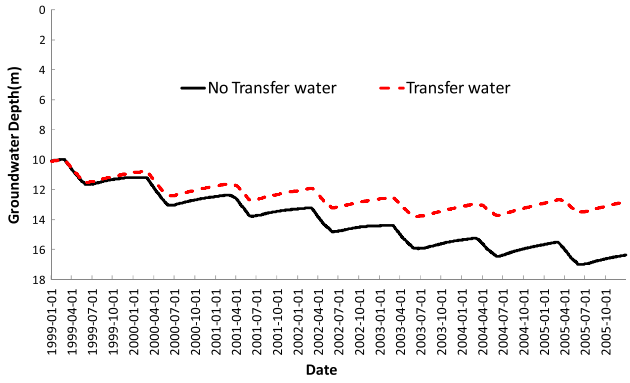

Figure 12. Average water table depth in Hai River plain region after transferring 9.5 billion m^3 of water

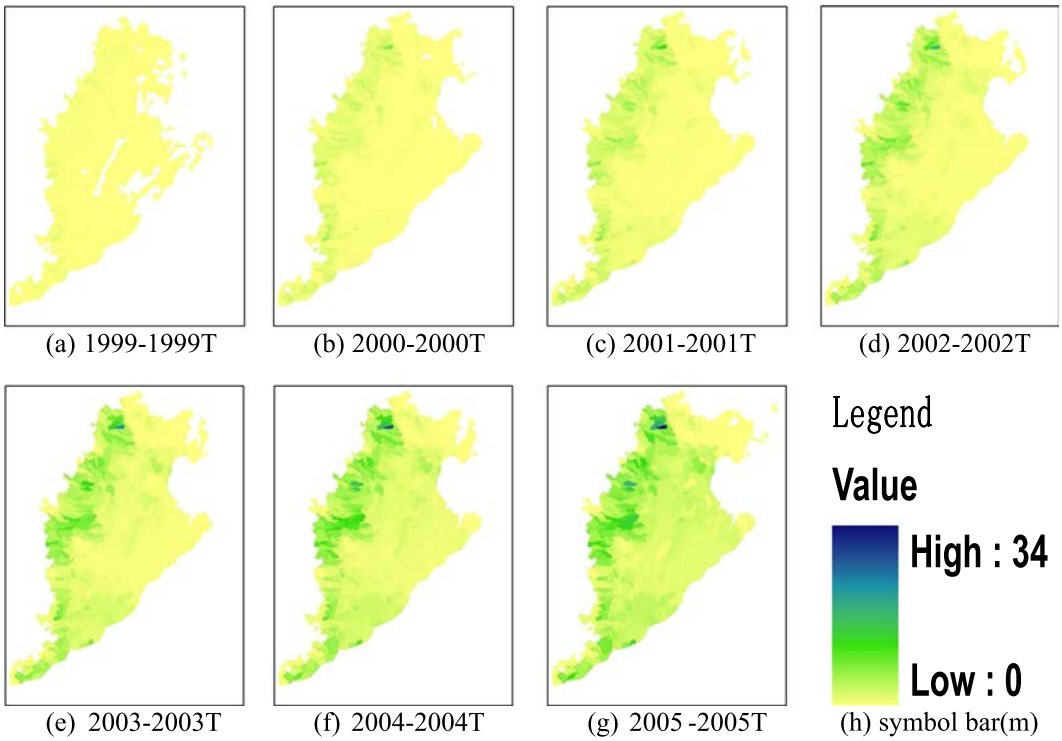

Figure 11. The difference in simulated annual water table depth between the two scenarios (with and without water transfer) in the Hai River plain. 'T' after the year refers to 'water transfer'

decrease the pumped groundwater and slow down groundwater level (Tables IV and V). At first, the CPT takes water directly to a nearby city. Thus, groundwater level changes are evident in areas near CTP. After transferring water for a long time, the whole basin groundwater level will change, because a basin is a system that is connected by surface water and groundwater.

The average groundwater depth (Figures 11 and 12) will continue to decline but at a slower rate (Table V).

CONCLUSIONS

To assess the impact of the central route of the CTP on the groundwater table, this study applied a large-scale surface-groundwater distributed hydrological model. The new model can solve the scale problem of coupling SWM and GWM. For the case study in the Hai River basin, the coupled model calculated surface run-off at first. At the same time, it can simulate the spatial–temporal distribution and change of the groundwater table. The model can also simulate groundwater pumping, water use and supply. There is a good match between simulated and observed hydrological values. Thus, the model is feasible and reasonable in water exchange between surface and groundwater.

Using this model, we quantitatively analysed the hydrological impact of CTP. The simulated results show that CTP only decreases rate of groundwater level decline and cannot fully resolve the water resource crisis in the Hai River basin. After transferring water, however, the groundwater overexploitation region will decline by approximately 20%, and the groundwater funnel area will also decline.

The results and tools presented previously are highly important for the CTP management, as transferred water will be a key water source for the Hai River basin. We need to better predict the potential CPT's impact and minimize the negative impact on groundwater.

ACKNOWLEDGMENTS

This study was supported by the CRSRI Open Research Program (Program: CKWV2012324/KY) and National science and technology support plan Program (NO. 2013BAB05B04).

REFERENCES

Arnold JG, Williams JR. 1997. *Model Theory of SWAT*. Agricultural Research Service Grassland: USA.

Barthel R, Rojanschi V, Wolf J, Braun J. 2005. Large-scale water resources management within the framework of GLOWA-Danube. Part a: the groundwater model. *Physics and Chemistry of the Earth*, Parts A/B/C, **30**(6–7): 372–382.

Beven KJ. 2001. *Rainfall-Runoff Modelling*. John Wiley & Sons Ltd: Chichester; 136–145, 162–166, 176~285.

Chen C. 2002. *The Problem of Numerical Simulation of the Ground Water Flows*. China University of Geosciences Press: Wuhan.

Chen F, Xie Z. 2010. Effects of interbasin water transfer on regional climate: a case study of the middle route of the South-to-North Water Transfer Project in China. *Journal of Geophysical Research: Atmospheres* **115**(D11): D11112.

Cui Y, Wang Y, Shao J, Chi Y, Lin L. 2009. Research on groundwater regulation and recovery in North China Plain after the implementation of south-to-north water transfer. *Resources Science* **31**(3): 382–387.

Cunningham AB, Sinclair PJ. 1979. Application and analysis of a coupled surface and groundwater model. *Developments in Water Science* **12**: 129–148.

Fleckenstein JH, Krause S, Hannah DM, Boano F. 2010. Groundwater-surface water interactions: new methods and models to improve understanding of processes and dynamics. *Advances in Water Resources* **33**(11): 1291–1295.

Garay HL, Haimes YY, Das P. 1976. Distributed parameter identification of groundwater systems by nonlinear estimation. *Journal of Hydrology* **30**(1–2): 47–61.

Harbaugh AW, McDonald MG. 1996. User's documentation for MODFLOW-96: an update to the USGS modular finite-difference ground-water flow model. *US Geological Survey Open File Report*: 96–485.

Kim NW, Chung IM, Won YS, Arnold JG. 2008. Development and application of the integrated SWAT-MODFLOW model. *Journal of Hydrology* **356**: 1–16.

Lautz LK, Siegel DI. 2006. Modeling surface and ground water mixing in the hyporheic zone using MODFLOW and MT3D. *Advances in Water Resources* **29**(11): 1618–1633.

Liu C, Zheng H. 2002. South-to-north water transfer schemes for China. *International Journal of Water Resources Development* **18**(3): 453–471.

Liu J, Zheng C, Zheng L, Lei Y. 2008. Ground water sustainability: methodology and application to the North China Plain. *Ground Water* **46**(6): 897–909.

Liu J, Qin D, Wang H, Wang M, Yang Z. 2010. Dualistic water cycle pattern and its evolution in Hai River basin. *Chinese Science Bulletin* **55**: 1688–1697.

Lubczynski WM, Gurwin J. 2005. Integration of various data sources for transient groundwater modeling with spatio-temporally variable fluxes —Sardon study case, Spain. *Journal of Hydrology* **306**(1–4): 71–96.

Maxwell RM, Miller NL. 2005. Development of a coupled land surface and groundwater model. *Journal of Hydrometeorology* **6**: 233–247.

Rodriguez LB, Cello PA, Vionnet CA, Goodrich D. 2008. Fully conservative coupling of HEC-RAS with MODFLOW to simulate stream-aquifer interactions in a drainage basin. *Journal of Hydrology* **353**(1–2): 129–142.

Shao J, Cui Y, Wang R, Li C, Yang Q. 2009. Groundwater modeling and evaluation in North China Plain. *Resources Science* **31**(3): 361–367.

Stone R, Jia H. 2006. Going against the flow. *Science* **313**(5790): 1034–1037.

Tang G, Alshawabkeh AN. 2006. A semi-analytical time integration for numerical solution of Boussinesq equation. *Advances in Water Resources* **29**: 1953–1968.

Wei S, Yang H, Abbaspour K, Mousavi J, Gnauck A. 2010. Game theory based models to analyze water conflicts in the middle route of the South-to-North Water Transfer Project in China. *Water Research* **44**(8): 2499–2516.

Wondzell SM, LaNier J, Haggerty R. 2009. Evaluation of alternative groundwater flow models for simulating hyporheic exchange in a small mountain stream. *Journal of Hydrology* **364**(1–2): 142–151.

Xia J. 2002. *Hydrological Nonlinear Theories and Approaches*. Wuhan University Press: Wuhan.

Xia J, Chen YD. 2001. Water problems and opportunities in the hydrological sciences in China. *Hydrological Sciences Journal* **46**(6): 907–921.

Xia J, Liu M, Jia S, Song X, Luo Y, Zhang S. 2004. Water security problem and research perspective in north China. *Journal of Natural Resources* **19**(5): 550–560.

Xia J, Wang G, Tan G, Hang G. 2005. Development of distributed time-variant gain model for nonlinear hydrological systems. *Science In China Series D: Earth Sciences* **48**(6): 26–28.

Xia J, Zhang L, Liu C, Yu J. 2007. Towards better water security in north China. *Water Resources Management* **21**(1): 233–247.
Xu K, Milliman JD, Xu H. 2010. Temporal trend of precipitation and runoff in major Chinese rivers since 1951. *Global and Planetary Change* **73**(3–4): 219–232.
Yang Y, Tian F. 2009. Abrupt change of runoff and its major driving factors in Haihe River Catchment, China. *Journal of Hydrology* **374**(3–4): 373–383.
Ye A, Xia J, Wang G. 2005. Drainage network extraction and subcatchment delineation based on digital elevation model. *Journal of Hydraulic Engineering* **36**(5): 531–537.
Ye A, Xia J, Wang G. 2006. A distributed kinematic routing model based on dynamical networks, *Yellow River* **2**: 26–28.
York JP, Person M, Gutowski WJ, Winter TC. 2002. Putting aquifers into atmospheric simulation models: an example from the Mill Creek Watershed, northeastern Kansas. *Advances in Water Resources* **25**(2): 221–238.
You J, Gan H, Tang K, Jia L, Niu C. 2011. Analysis of impact of South-to-North Water Transfer Project on groundwater exploitation in north China. *Paper presented at the EWRI Congress 2011*, Palm Springs, CA, United states.
Zhao RJ. 1992. The Xinanjiang model applied in china. *Journal of Hydrology* **35**(1–4): 371–381.
Zheng J, Dou Y, Shao J, Cui Y. 2009. Prediction of groundwater flow field in the west suburb of Beijing before and after the South-to-North Water Diversion. *Geotechnical Investigation & Surveying* **5**: 35–39.
Zhong H, Bian J, Li W. 2010. Groundwater protection and remediation measures for the water imported areas of the South-to-North water diversion. *China water resources* **7**: 33–35.

APPENDIX A: MODEL DESCRIPTION

SWM – Distributed Time-Variant Gain Hydrological Model

We select the Distributed Time-Variant Gain Hydrological Model (DTVGM) to calculate surface water. The TVGM is a rainfall-run-off modelling system developed on the basis of non-linear Volterra functional series and a conceptual hydrological modelling approach (Xia, 2002; Xia *et al*., 2005). With the adoption of geographic information system technology, TVGM is extended to include a distributed hydrologic modelling capability (DTVGM).

The DTVGM, combining the advantages of both non-linear and distributed hydrologic models, can simulate various hydrologic processes under different environmental conditions. Promising results were obtained in forecasting the time–space variations of hydrologic processes and the relationships between land use/land cover change and surface run-off variation.

The DTVGM (Xia *et al*., 2005) is a conservation model of water. On the basis of sub-basins, which are divided from large basins, run-off calculated in each sub-basin and routing is calculated among sub-basins.

Run-off method

Run-off is calculated for each hydrologic unit (i.e. sub-basin or grid). There are three layers in the model: vegetation layer, surface soil layer and deep soil layer. There are three run-off components: surface run-off on land surface, sub-surface run-off from the surface soil layer and base flow from the deep soil layer.

The DTVGM is basically a water balance model. Evaporation, soil moisture and run-off are computed iteratively. The water balance equation is

$$P_i + W_i = W_{i+1} + Rs_i + Rss_i + Rg_i + E_i \qquad \text{(A.1)}$$

where P is precipitation, W is soil moisture, Rs is surface run-off, Rss is sub-surface run-off, Rg is groundwater run-off, E is evaporation and i is period of time.

Inserting current evaporation, surface run-off, sub-surface run-off and base flow in Equation 1, we obtain

$$P_i + W_i = W_{i+1} + g_1\left(\frac{W_{ui}}{WM_u \cdot C_j}\right)^{g_2} P + W_{ui} \cdot K_r + f_c \cdot \left(\frac{W_{gi}}{WM_g}\right)^{K_g} + Ep_i \cdot \left(\frac{W_{ui}}{WM_u \cdot C_j}\right) \qquad \text{(A.2)}$$

where W is soil moisture (mm), W_u is the upper soil moisture at the sub-basin (mm), W_g is the lower soil moisture at the sub-basin (mm), WM_u is the upper saturated soil moisture (mm), u is the 'upper' soil, WM_g is the lower saturated soil moisture (mm), f_c is the soil permeability coefficient (mm/h), g_1 and g_2 are parameters ($0 < g_1 < 1$, $0 < g_2$), g_1 is the run-off coefficient when the soil is saturated, g_2 is the soil moisture parameter, C is the land cover parameter, K_r is the sub-surface run-off coefficient, K_g is the groundwater run-off coefficient, K_e is the evaporation coefficient, i is a period of time and j is the hydrological unit number.

Routing model

The routing model used is the kinematic wave model. To simplify the model, the friction term in the momentum equation is ignored. Assuming that the friction slope (Sf) is equal to the ground slope ($S0$), and the river flow is gradually varying unsteady flow in open channels (Ye *et al*., 2006), the continuity equation is written as

$$\frac{\partial A}{\partial t} + \frac{\partial Q}{\partial x} = q \qquad \text{(A.3)}$$

where A is the river cross section area (m^2), t is time (s), Q is discharge (m^3/s), x is the flow path (m) and q is the lateral inflow (m^2/s).

Flow velocity (v, m/s) is calculated on the basis of the Manning formula:

$$v = \frac{1}{n} \cdot h^{\frac{2}{3}} S_0^{\frac{1}{2}} \qquad \text{(A.4)}$$

where n is the Manning roughness coefficient, and S_0 is slope.

The discharge at the river cross section is

$$Q = A \cdot v \tag{A.5}$$

The river stream network is encoded from the outlet of the basin to upstream (Figure A. A) (Ye *et al*., 2005). The routing is calculated from upstream to the basin outlet.

There are five sub-models regarding human activity: domestic water use, industrial water use, agricultural irrigation water use, water transfer and reservoir operation.

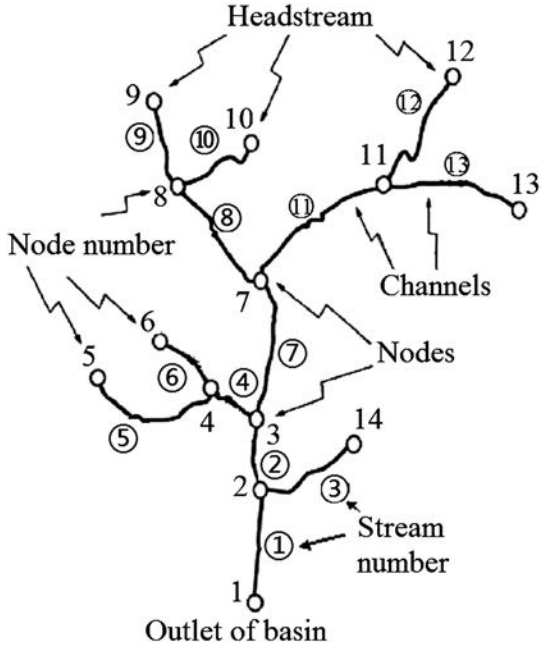

Figure A.1. Sketch map of the stream network definition

Groundwater table calculation in the grid

The Dupuit assumption holds that groundwater moves horizontally in an unconfined aquifer and that the groundwater discharge is proportional to the saturated aquifer thickness. The assumption was first proposed by Jules Dupuit in 1863 to simplify the groundwater flow equation for analytical solutions (Chen, 2002). This paper simplifies the three dimensions in the groundwater flow equation to a two-dimensional equation.

The Boussinesq equation is a two-dimensional equation (Tang and Alshawabkeh, 2006):

$$\frac{\partial}{\partial x}\left(k_{xx}(H-Z)\frac{\partial H}{\partial x}\right)+\frac{\partial}{\partial y}\left(k_{yy}(H-Z)\frac{\partial H}{\partial y}\right)+\varepsilon=\mu_d\frac{\partial H}{\partial t} \tag{A.6}$$

where H is the elevation of the phreatic surface above the datum (m); Z is the elevation of the unconfined aquifer's bottom above the datum (m); k_{xx} and k_{yy} are the hydraulic conductivities in x and y, respectively (m/day); μ is the specific yield; ε is the infiltration rate (m/day) and x, y and t are the space (m) and time coordinates (day).

To simplify the model and decrease its computation time, the model assumed each grid has four flow directions, that is, only four neighbour grids exchange water with the current grid (Figure A. 2). The flow direction of each grid can be determined by the groundwater table level and hydraulic conductivities k. The flow direction heads towards low-pressure spots, but the structure of the rock may change the flow direction. Hydraulic conductivity is an index that confirms the flow direction in all grids.

Water balance and groundwater table calculated in each grid

The groundwater level changed very slowly. Each grid calculated the water balance by the Boussinesq equation (Figure A.3).

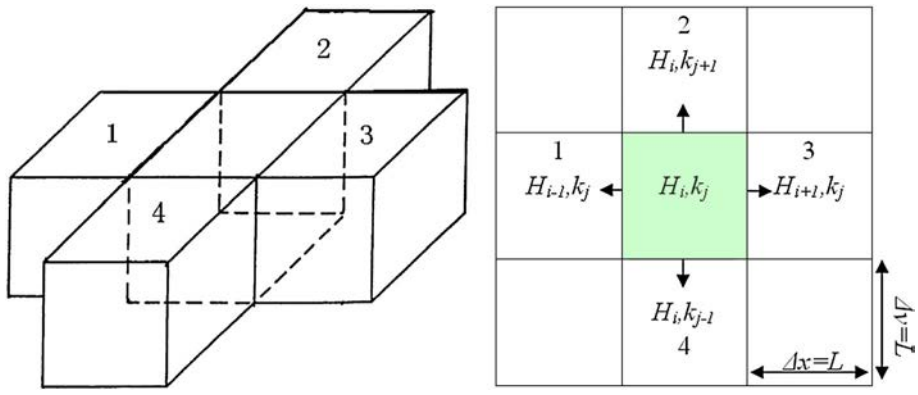

Figure A.2. Flow direction of each of the four neighbour grids. H is groundwater table. k is hydraulic conductivity. i and j are grid numbers. L is the length of the grid side

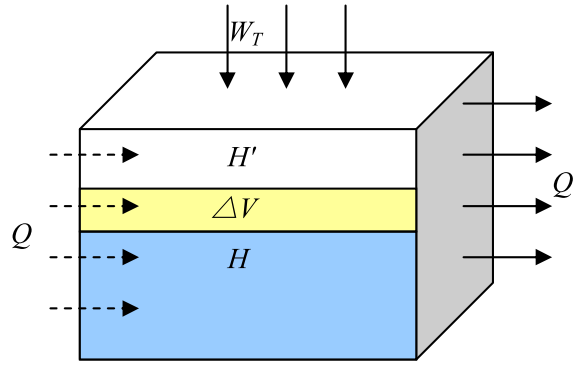

Figure A.3. Two-dimensional model of groundwater. Q is lateral discharge. W_T is water exchange between groundwater and surface water. H is initial groundwater table. H' is final groundwater table. $\triangle V$ is storage change variation of groundwater

The four neighbours' discharges of each grid (Figure 5) are

$$Q_i = F_i \cdot v_i = H_t \cdot L \cdot k_i \cdot \frac{H - H_i}{L} \qquad (i = 1, 2, 3, 4) \quad \text{(A.7)}$$

where Q is discharge (m^3/s), i is the grid number, F is river cross section area (m^2), v is the flow rate (m/s), H_t is the depth of the saturated zone (m), k is hydraulic conductivity (m/day), H is the groundwater level (m) and L is the grid width (m).

$$\begin{aligned} &\sum_{i=1}^{4} Q_i \cdot \Delta t + W_T = \mu \cdot \Delta H \cdot L^2 \\ &\Rightarrow \sum_{i=1}^{4} H_t \cdot L \cdot k_i \cdot \frac{H - H_i}{L} \cdot \Delta t + W_T = \mu \cdot \Delta H \cdot L^2 \\ &\Rightarrow \sum_{i=1}^{4} H_t \cdot k_i \cdot (H - H_i) \cdot \Delta t + W_T = \mu \cdot \Delta H \cdot L^2 \\ &\Rightarrow \Delta H = \frac{1}{\mu \cdot L^2} \left(\sum_{i=1}^{4} H_t \cdot k_i \cdot (H - H_i) \cdot \Delta t + W_T \right) \end{aligned} \qquad \text{(A.8)}$$

$$\Delta H = H' - H \Rightarrow H' = \Delta H + H \qquad \text{(A.9)}$$

where H is the current groundwater level (m), H' is the groundwater level for the next time interval (m) and ΔH is the change of the water level (m).

Human activities in the model

Human activities, including irrigation, domestic and industrial water uses, are calculated in the model.

Agricultural irrigation water is determined by the irrigation area and crop species. Taking feasibility and practicability into consideration, this article employs the formula in the succeeding texts to simulate the agricultural water demand Irw (m^3).

$$Irw = \alpha_j \beta S_1 \qquad \sum_{j=1}^{12} \alpha_j = 1 \qquad \text{(A.10)}$$

where α_j denotes the agricultural water consumption ratio of each month, determined by the irrigation period ($j = 1,2,\ldots\ldots12$); β denotes the annual water consumption per unit area of agriculture (mm), determined by the types of crops and irrigation methods and generally have measured data and S_1 denotes the cultivated land area (km^2).

It is difficult for hydrological models to obtain the real-time actual industrial water consumption statistics of the basin, especially when they are applied in large basin, as gross domestic product (GDP) has good correlation with industrial water consumption, and the statistics of the industrial GDP of each region as well as the water consumption of per unit GDP are available. We estimate industrial water consumption of each hydrological unit by GDP here.

$$Inw = GDP \cdot GDPN \qquad \text{(A.11)}$$

where Inw is the industrial water demand (m^3), GDP is gross domestic product (\$) and $GDPN$ is the water consumption of per unit GDP (m^3/\$). The spatial distributions of $GDPN$ create a gap between different hydrological units, because of the differences between the industrial water consumption of different regions. That is to say, the mean $GDPN$ in each hydrological unit is varied.

Domestic water consumption refers to water consumption in daily life. The domestic water consumption was identified by the population, as there is a high correlation between domestic water consumption and population.

$$Dow = Po \cdot PN \qquad \text{(A.12)}$$

$$Do = Dow \cdot \varphi L \qquad \text{(A.13)}$$

Where Dow is domestic water demand (m^3), Do is domestic water consumption, Po is the number of population, PN is water consumption per capita, φI is the water return coefficient of domestic water consumption.